Prestack Stolt residual migration for migration velocity analysis

Paul Sava, Stanford University

SUMMARY

This paper presents a method of Stolt residual migration applicable to prestack data. The method's main merit is that instead of requiring an assumption about the magnitude of the new velocity model to which we want to residually migrate, it only calls for an assumption about the ratio of the reference velocity to the new one. Since the method is, in essence, a Stolt-stretch technique, it inherits Stolt's speed and convenience. I evaluate the quality of migration, and implicitly the quality of residual migration, using angle-domain common-image gathers. Two examples show that the method can be successfully used in residual migration even when the reference velocity is not constant. An important application of the method is in the area of wave-equation migration velocity analysis.

INTRODUCTION

Residual migration has proved to be a useful tool in imaging and in migration velocity analysis.

Rothman (1985) shows that post-stack residual migration can be successfully used to improve the focusing of the migrated sections. He also shows that migration with a given velocity (v) is equivalent to migration with a reference velocity (v_0) followed by residual migration with a velocity (v_r) that can be expressed as a function of v_0 and v.

Residual migration has also been used as a tool in velocity analysis. Al-Yahya and Fowler (1986; 1987) discuss a residual migration operator in the prestack domain, and show that it can be posed as a function of a non-dimensional parameter (γ) that is the ratio of the correct velocity and the reference velocity used for the initial migration. Etgen (1988; 1989) defines a kinematic residual migration operator as a cascade of NMO and DMO, and shows that it, again, is only a function of the non-dimensional parameter (γ) defined by Al-Yahya. Finally, Stolt (1996) defines a prestack residual migration operator in the (ω,k) domain, and shows that it depends on the reference (v_0) and the correct (v) migration velocities, but not on a residual velocity (v_r) as in the post-stack case.

In this paper, I review the prestack Stolt residual migration, showing that it also can be formulated as a function of a non-dimensional parameter that is the ratio of the reference (v_0) and correct (v) velocities. Consequently, we can use Stolt residual migration in the prestack domain to obtain a better-focused image without making assumptions about the velocity magnitude. This approach has a direct application to migration velocity analysis, when we repeatedly need to do residual migration on images that have been depth-migrated with an arbitrary velocity function (Biondi and Sava, 1999).

THEORY

This section introduces the theory of Stolt residual migration in the prestack domain. I begin with a short discussion of Stolt migration, then derive the equations for Stolt prestack residual migration of 3D, 2D and 3D common-azimuth data.

Stolt Migration

Prestack Stolt migration can be summarized (Claerbout, 1985) as a succession of transformations from seismic data $(d,\mathcal{D})$ to seismic images $(r,\mathcal{R})$ as

$$d(t,\vec{m},\vec{h}) \rightarrow \mathcal{D}(\omega,\vec{k}_m,\vec{k}_h) \rightarrow \mathcal{R}(k_z,\vec{k}_m,\vec{k}_h) \rightarrow r(z,\vec{m},\vec{h}).$$

An important component of prestack Stolt migration is the re-mapping from the $(\omega,\vec{k}_m,\vec{k}_h)$ domain to the $(k_z,\vec{k}_m,\vec{k}_h)$ domain, where ω, k_z represent, respectively, the frequency and the vertical wavenumber, and $\vec{k}_m,\vec{k}_h$ represent the midpoint and offset wavenumbers.

If we consider the representation of the input data in shot-geophone coordinates, the mapping takes the form

$$k_z = \frac{1}{2}\sqrt{\frac{\omega^2}{v^2}-|\vec{k}_g|^2}+\frac{1}{2}\sqrt{\frac{\omega^2}{v^2}-|\vec{k}_s|^2}, \tag{1}$$

where $\vec{k}_g$ and $\vec{k}_s$ stand for, respectively, the geophone and the source wavenumbers. We can, therefore, express ω as a function of k_z from Equation (1) as

$$\omega^2 = v^2\frac{\left[4k_z^2+\left(|\vec{k}_g|-|\vec{k}_s|\right)^2\right]\left[4k_z^2+\left(|\vec{k}_g|+|\vec{k}_s|\right)^2\right]}{16k_z^2} \tag{2}$$

We can obtain an equation equivalent to (2) in midpoint-offset coordinates, if we make the usual change of variables:

$$\begin{aligned}\vec{k}_g &= \vec{k}_m+\vec{k}_h\\ \vec{k}_s &= \vec{k}_m-\vec{k}_h.\end{aligned} \tag{3}$$

Stolt Residual Migration

In general, residual migration represents a method of improving the quality of the image that does not require re-migration of the original data, but, rather, only a transformation applied to the current migrated image.

In prestack Stolt residual migration, we attempt to correct the effects of migrating with an inaccurate reference velocity by applying a transformation to the images that have been transformed to the Fourier domain (Figure 1). Supposing that the initial migration was done with the velocity v_0, and that the correct velocity is v, we can use Equation (1) to derive k_{z_0}, the vertical wavenumber for the reference velocity, and k_z, the vertical wavenumber for the correct velocity.

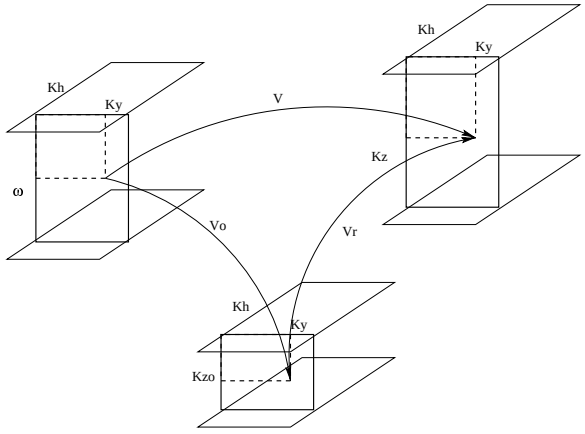

Figure 1: A sketch of Stolt residual migration.

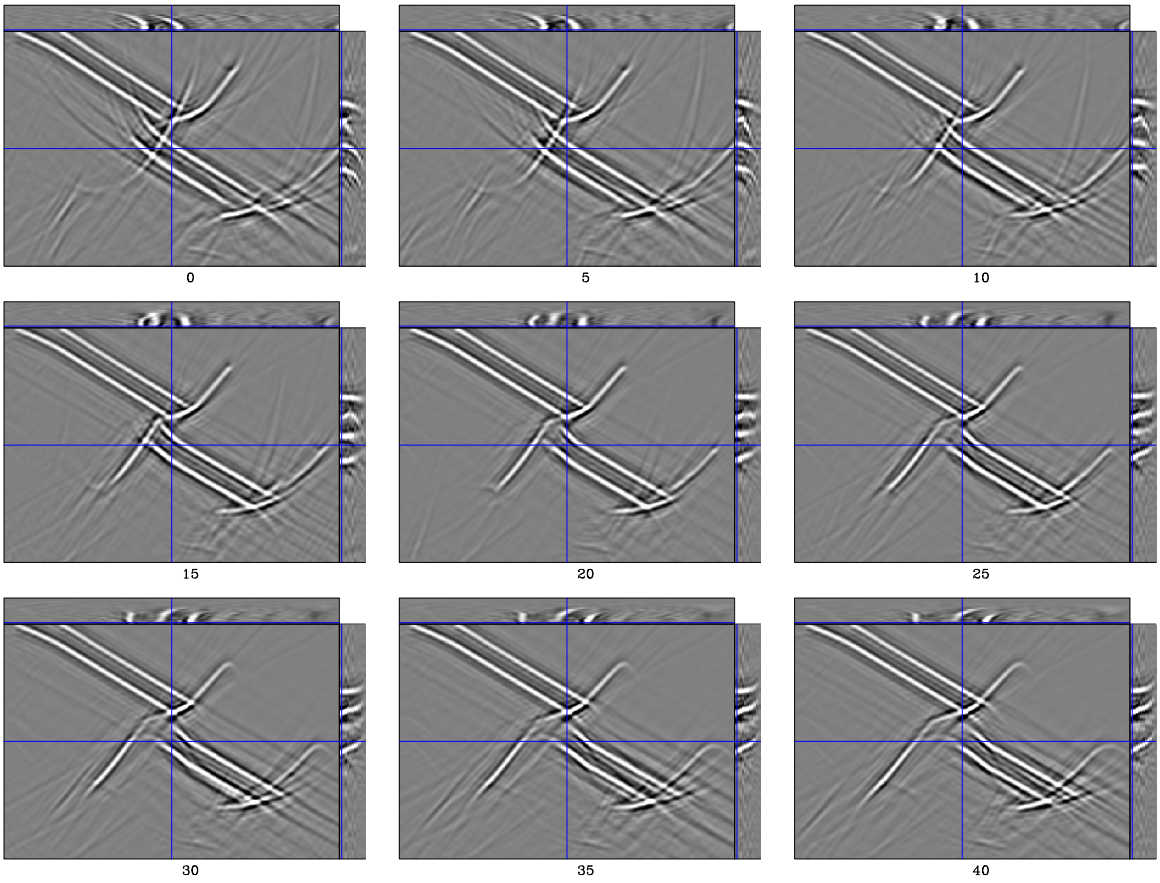

Figure 2: Residual migration images. Each panel corresponds to a different residual migration ratio (γ), as follows: 0($\gamma = 0.9$), 5($\gamma = 0.925$), 10($\gamma = 0.95$), 15($\gamma = 0.975$), 20($\gamma = 1.0$), 25($\gamma = 1.025$), 30($\gamma = 1.05$), 35($\gamma = 1.075$), 40($\gamma = 1.1$). The values of γ smaller than 1.0 correspond to new velocities that are higher than the original, while the values above 1.0 correspond to new velocities lower than the original. The panel labeled 20 is the original image with no residual migration ($\gamma = 1.0$).

Mathematically, the goal of prestack Stolt residual migration is to obtain k_z from k_{z_0}. If we substitute ω from k_{z_0} to k_z, we obtain the residual migration equation for full 3D prestack seismic images:

$$k_z = \frac{1}{2}\sqrt{\frac{v_0^2}{v^2}\frac{\left[4k_{z_0}^2+\left(|\vec{k}_g|-|\vec{k}_s|\right)^2\right]\left[4k_{z_0}^2+\left(|\vec{k}_g|+|\vec{k}_s|\right)^2\right]}{16k_{z_0}^2}-|\vec{k}_g|^2} + \frac{1}{2}\sqrt{\frac{v_0^2}{v^2}\frac{\left[4k_{z_0}^2+\left(|\vec{k}_g|-|\vec{k}_s|\right)^2\right]\left[4k_{z_0}^2+\left(|\vec{k}_g|+|\vec{k}_s|\right)^2\right]}{16k_{z_0}^2}-|\vec{k}_s|^2}, \tag{4}$$

which can also be represented in midpoint-offset coordinates using the change of variables in Equation (3).

In the 3D post-stack case, when $\vec{k}_h = \vec{0}$, Equation (4) becomes:

$$k_z = \sqrt{\frac{v_0^2}{v^2}\left[k_{z_0}^2+|\vec{k}_m|^2\right]-|\vec{k}_m|^2}. \tag{5}$$

In the 2D prestack case, if we define the components of the midpoint and offset wavenumbers as $\vec{k}_m = (k_{mx}, k_{my})$ and $\vec{k}_h = (k_{hx}, k_{hy})$, we can write Equation (4) as:

$$k_z = \frac{1}{2}\sqrt{\frac{v_0^2}{v^2}\frac{\left[k_{z_0}^2+k_{hx}^2\right]\left[k_{z_0}^2+k_{mx}^2\right]}{k_{z_0}^2}-(k_{mx}+k_{hx})^2} + \frac{1}{2}\sqrt{\frac{v_0^2}{v^2}\frac{\left[k_{z_0}^2+k_{hx}^2\right]\left[k_{z_0}^2+k_{mx}^2\right]}{k_{z_0}^2}-(k_{mx}-k_{hx})^2}. \tag{6}$$

For 2D post-stack data, Equation (6) becomes

$$k_z = \sqrt{\frac{v_0^2}{v^2}\left[k_{z_0}^2+k_{mx}^2\right]-k_{mx}^2}, \tag{7}$$

which can also be written in the familiar form (Stolt, 1996):

$$\omega = \sqrt{\omega_0^2+k_{mx}^2\left(v_0^2-v^2\right)} \tag{8}$$

Common-azimuth Stolt Residual migration

Common-azimuth data represent subsets of 3D datasets that have been recorded or transformed to zero cross-line offsets ($h_y = 0$). Stolt migration for common-azimuth data involves the use of the dispersion relation (Biondi and Palacharla, 1996)

$$k_{zx} = \frac{1}{2}\sqrt{\frac{\omega^2}{v^2}-(k_{mx}-k_{hx})^2}+\frac{1}{2}\sqrt{\frac{\omega^2}{v^2}-(k_{mx}+k_{hx})^2}, \tag{9}$$

where the depth wavenumber of the common-azimuth dataset (k_z) is written as

$$k_z = \sqrt{k_{z_x}^2 - k_{m_y}^2}. \tag{10}$$

We can re-write Equations (9) and (10) for a given reference velocity (v_0) and obtain the corresponding depth wavenumbers $k_{z_{x0}}$ and k_{z_0}. Mathematically, the goal of common-azimuth Stolt residual migrations is to obtain k_z from k_{z_0}. Again, we can achieve this by eliminating the frequency ω from k_{z_0} and k_z, which leads to the 3D common-azimuth residual migration equations:

$$\begin{cases} k_{z_x} = \frac{1}{2}\sqrt{\frac{v_0^2}{v^2}\frac{\left[k_{z_0}^2+k_{m_y}^2+k_{h_x}^2\right]\left[k_{z_0}^2+k_{m_y}^2+k_{m_x}^2\right]}{k_{z_0}^2+k_{m_y}^2} - \left(k_{m_x}-k_{h_x}\right)^2} \\ \qquad +\frac{1}{2}\sqrt{\frac{v_0^2}{v^2}\frac{\left[k_{z_0}^2+k_{m_y}^2+k_{h_x}^2\right]\left[k_{z_0}^2+k_{m_y}^2+k_{m_x}^2\right]}{k_{z_0}^2+k_{m_y}^2} - \left(k_{m_x}+k_{h_x}\right)^2} \\ k_z = \sqrt{k_{z_x}^2 - k_{m_y}^2} \end{cases} \tag{11}$$

For 2D data, when $k_{m_y} = 0$, $k_z \equiv k_{z_x}$ and $k_{z_0} \equiv k_{z_{x0}}$, the Equations (11) reduce to the 2D prestack (6) and post-stack (7) forms.

Angle-domain common-image gathers

Angle-domain common-image gathers are representations of the seismic images sorted by the aperture angle at the reflection point (Prucha et al., 1999). Such representations can be used to evaluate the quality of the migrated image: the migration is correct if the events are flat along the angle axis; it is incorrect otherwise.

The angle-domain common-image gathers can be computed in the Fourier domain using the simple relation

$$\tan\alpha = -\frac{|\vec{k}_h|}{k_z}, \tag{12}$$

where α represents the reflection angle at the reflector.

DISCUSSION

From the theory presented in the preceding sections, we can conclude that prestack Stolt residual migration can be done without making an assumption about the new velocity to which we residually migrate the data, but, rather, by selecting a ratio of the current velocity to the new one ($\gamma = v_0/v$). This conclusion is true in the 3D case (Equations 4 and 5), the 2D case (Equation 6 and 7), and the case of 3D common-azimuth data (Equation 11).

Stolt (1996) comments that, in the post-stack case, the frequency after time migration can be related to the frequency of the original data and the difference of the squares of the two velocities, before and after residual migration (Equation 8). However, Stolt shows that such a conclusion is not true anymore in the prestack case. Still, if we reformulate Stolt residual migration for depth-migrated data, we can do residual migration by taking the ratios of the velocities instead of their difference, which is even better, since in most cases the original image has not been migrated with a constant velocity.

EXAMPLES

I will illustrate the residual migration technique with two 2D synthetic examples.

The first is a simple model with a fast velocity layer embedded in a slower background. Figure 2 shows the results of residual migration applied to the images for different values of the velocity ratios (γ). The image labeled 20 corresponds to the original image without residual migration. The other frames correspond to other values of γ, both lower and higher than 1, which indicate both over and under-migration. The angle-domain common-image gathers show the degree to which each event departs from the correct position. Ideally, all the events should be flat, but as we can see, each one flattens best at a different ratio, since the velocity model is variable. Finally, from all the images at different ratios, we can interpolate an optimal one, which displays the best flattened image gathers at all locations, measured by the magnitude of the stack along the angle direction (Figure 3).

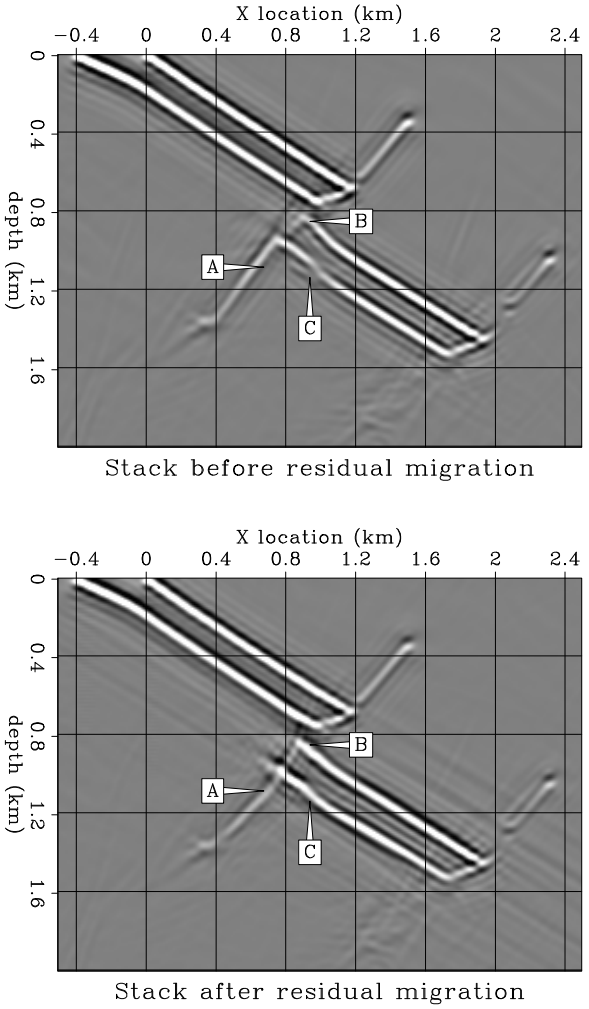

Figure 3: A comparison between the original image obtained through migration with the wrong velocity and the improved image obtained after residual migration. The area of interest is located at the horizontal location $0.7-1.1$ km and depth $0.8-1.0$ km. The segment of the fault in the shadow of the fast layer is moved to the right toward its correct position (A). The reflectors B and C, also in the shadow of the fast layer, are moved almost to their correct position and are much more energetic in the best-focused image (below) than in the original image (above).

The second example is represented by a synthetic model in a salt dome region (Figure 4). The top panel shows the image obtained using a good estimate of the velocity model. Most of the events, especially in the upper part of the model, display flat angle-domain common-image gathers. However, if we used a wrong velocity model, a scaled version of the original, we would get an incorrectly migrated image (middle panel), characterized by upward-pointing

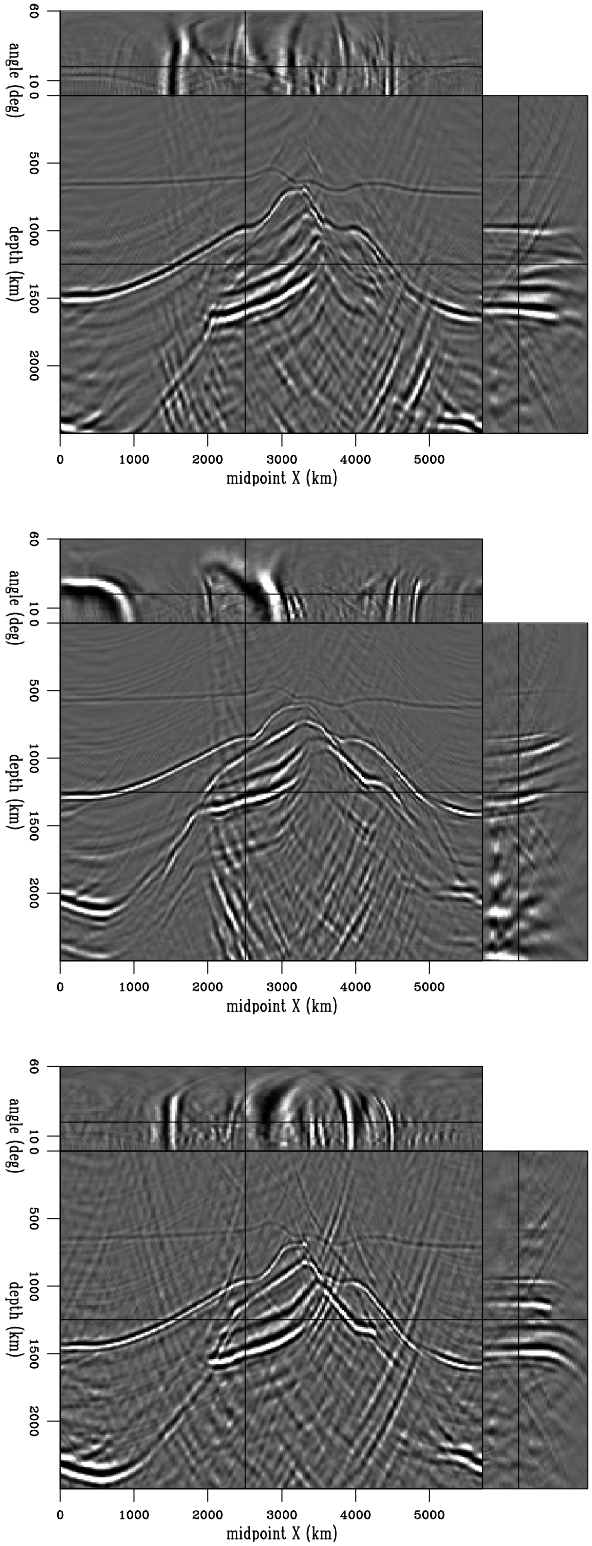

Figure 4: An example of prestack Stolt residual migration. The top panel represents the image obtained using the true velocity model. The middle panel represents the migration result in the case where we scale down the velocity model with a factor $\gamma = 0.9$. Most of the events are thus not migrated correctly, as shown by the angle-domain common-image gathers that are pointing upward. The bottom panel represents the result of residual migration using 0.9 as the velocity ratio. Most of the events are flattened back to their correct position.

events on the angle axis. Finally, residual migration with the appropriate ratio restores most of the correct image (lower panel).

CONCLUSIONS

This paper shows that we can reformulate prestack Stolt residual migration for depth migrated images. In essence, the residual migration introduced here is a Stolt-stretch method; therefore, it retains both the advantages and the disadvantages of the Stolt-type techniques.

The main benefit of this method is that we can residually migrate without making assumptions about the magnitude of the new velocities directly, but rather by assuming different ratios of the current to the new velocity. In this way, we can apply Stolt residual migration to images that have been migrated with an arbitrary velocity map, and not only to those migrated with constant velocity. This conclusion is valid for all types of seismic images, from 2D post-stack, to 3D prestack, including 3D common-azimuth.

Because the method discussed here is cheap, an important application of it could be in the area of repeated residual image enhancement. Consequently, the method could be employed in wave-equation migration velocity analysis, where we need to evaluate the difference between an enhanced image and the reference one, a difference from which we could update the velocity map (Biondi and Sava, 1999).

ACKNOWLEDGMENTS

The author would like to thank Elf Aquitaine for providing the data for the synthetic salt dome model used in this paper.

REFERENCES

Al-Yahya, K., and Fowler, P., 1986, Prestack residual migration: SEP–**50**, 219–230.

Al-Yahya, K., 1987, Velocity analysis by iterative profile migration: Ph.D. thesis, Stanford University.

Biondi, B., and Palacharla, G., 1996, 3-D prestack migration of common-azimuth data: Geophysics, **61**, no. 6, 1822–1832.

Biondi, B., and Sava, P., 1999, Wave-equation migration velocity analysis: 69th Ann. Internat. Meeting, Soc. Expl. Geophys., 1723–1726.

Claerbout, J. F., 1985, Imaging the Earth's Interior: Blackwell Scientific Publications.

Etgen, J., 1988, Velocity analysis by prestack depth migration : Linear theory: 58th Ann. Internat. Mtg., Soc. Expl. Geophys., Expanded Abstracts.

Etgen, J., 1989, Kinematic residual prestack migration: SEP–**61**, 79–102.

Prucha, M., Biondi, B., and Symes, W., 1999, Angle-domain common image gathers by wave-equation migration: 69th Ann. Internat. Meeting, Soc. Expl. Geophys., 824–827.

Rothman, D. H., Levin, S. A., and Rocca, F., 1985, Residual migration – applications and limitations: Geophysics, **50**, no. 1, 110–126.

Stolt, R. H., 1996, Short note–a prestack residual time migration operator: Geophysics, **61**, no. 2, 605–607.